Chemoenzymatic Synthesis of an Unnatural Deazaflavin Cofactor That Can Fuel F-420-Dependent Enzymes

Drenth, Jeroen; Trajkovic, Milos; Fraaije, Marco W.

Published in:
ACS Catalysis

DOI:
10.1021/acscatal.9b01506

Publication date:
2019

ACS Catalysis

Research Article

Cite This: ACS Catal. 2019, 9, 6435−6443

pubs.acs.org/acscatalysis

Chemoenzymatic Synthesis of an Unnatural Deazaflavin Cofactor That Can Fuel F_{420}-Dependent Enzymes

Jeroen Drenth, Milos Trajkovic, and Marco W. Fraaije*

Molecular Enzymology Group, University of Groningen, Nijenborgh 4, 9747AG Groningen, The Netherlands

Supporting Information

ABSTRACT: F_{420}-dependent enzymes are found in many microorganisms and can catalyze a wide range of redox reactions, including those with some substrates that are otherwise recalcitrant to enzyme-mediated reductions. Unfortunately, the scarceness of the cofactor prevents application of these enzymes in biocatalysis. The best F_{420}-producing organism, *Mycobacterium smegmatis*, only produces 1.4 μmol per liter of culture. Therefore, we synthesized the unnatural cofactor FO-5′-phosphate, coined FOP. The FO core-structure was chemically synthesized, and an engineered riboflavin kinase from *Corynebacterium ammoniagenes* (CaRFK) was then used to phosphorylate the 5′-hydroxyl group. The triple F21H/F85H/A66I CaRFK mutant reached 80% of FO conversion in 12 h. The same enzyme could produce 1 mg (2.5 μmol) of FOP in 50 mL of reaction volume, which translates to a production of 50 μmol/L. The activity toward FOP was tested for an enzyme of each of the three main structural classes of F_{420}-dependent oxidoreductases. The sugar-6-phosphate dehydrogenase from *Cryptosporangium arvum* (FSD-Cryar), the F_{420}:NADPH oxidoreductase from *Thermobifida fusca* (TfuFNO), and the F_{420}-dependent reductases from *Mycobacterium hassiacum* (FDR-Mha) all showed activity for FOP. Although the activity for FOP was lower than that for F_{420}, with slightly lower k_{cat} and higher K_m values, the catalytic efficiencies were only 2.0, 12.6, and 22.4 times lower for TfuFNO, FSD-Cryar, and FDR-Mha, respectively. Thus, FOP could be a serious alternative for replacing F_{420} and might boost the application of F_{420}-dependent enzymes in biocatalysis.

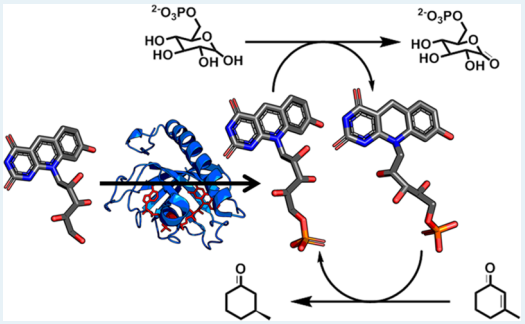

KEYWORDS: *deazaflavin, riboflavin kinase, F_{420}, biocatalysis, reductase*

INTRODUCTION

The naturally occurring cofactor F_{420} was discovered in 1972 in methanogenic archaea where it plays a crucial role in one-carbon catabolism.[1] Nowadays, F_{420} is known to be present in a wide range of archaea and bacteria in which it plays an important role in many processes as a redox cofactor.[2−5] In several Actinobacteria, for instance, it plays a crucial role in antibiotic synthesis,[6−8] as well as aflatoxin degradation,[5,9,10] and degradation of other aromatic compounds.[11−13] Also, the notorious pathogen *Mycobacterium tuberculosis* has a high abundance of F_{420}-dependent proteins.[4] In this organism, F_{420} is crucial in the regulation of oxidative and nitrosative stress.[14−16] Ironically, a series of antitubercular nitroimidazole prodrugs, like pretomanid (PA-824) and delamanid (OPC-67683), are specifically activated by a F_{420}-dependent reductase in vivo, releasing toxic NO.[17−19]

Structurally, the 7,8-didemethyl-8-hydroxy-5-deazariboflavin catalytic core of F_{420}, called FO, is analogous to that of riboflavin[20] (see Figure 1). Its chemistry, however, resembles more that of nicotinamide dinucleotide ($NAD(P)^+$), as F_{420} can only perform two-electron hydride transfers and is hardly reactive toward molecular oxygen. Its reduction potential of −360 mV is lower than that of $NAD(P)^+$ and the riboflavin derived cofactors flavin mononucleotide (FMN) and flavin adenine dinucleotide (FAD), which are −320 and −220 mV, respectively.[21] Apart from the FO core, the rest of the structure is very different than that of the nicotinamide and flavin cofactors. The ribityl tail of FO is extended with a 5′-phospho-L-lactyl moiety, forming F_{420}-0, and this is in turn elongated by

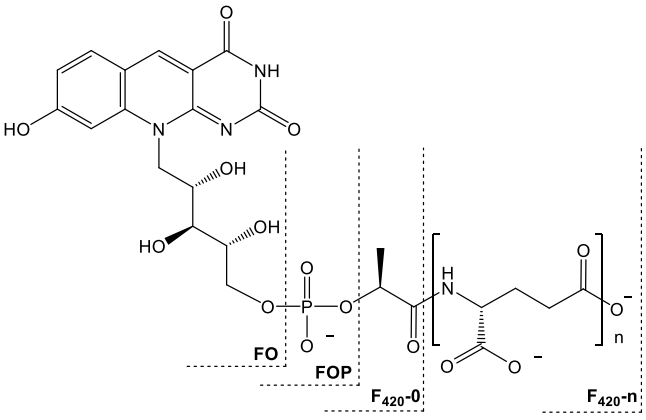

Figure 1. Structure of F_{420} and related compounds.

Received: April 12, 2019
Revised: June 4, 2019
Published: June 7, 2019

DOI: 10.1021/acscatal.9b01506
ACS Catal. 2019, 9, 6435−6443

a poly-γ-glutamyl tail.[20] The length of the poly-γ-glutamyl tail depends on the organism and varies from 2 to 9 monomers.[3,22] Interestingly, the larger part of the poly-γ-glutamyl tail is not bound to the enzyme, as was seen in several crystal structures and modeled protein structures.[9,23−28] Ney et al.,[3] however, showed that electrostatic interactions of the poly-γ-glutamyl tail with enzymes of the split β-barrel like fold flavin/deazaflavin oxidoreductase (FDOR) and TIM barrel fold luciferase-like hydride transferase (LLHT) families influences the binding affinity. It seems that a longer polyglutamyl tail results in a higher binding affinity (lower K_d and K_m), which lowers the catalytic turnover (k_{cat}), probably because of slower cofactor exchange rates.

The uniquely low redox potential of the cofactor makes it an interesting candidate for the use in biocatalysis.[29,30] F_{420}-dependent enzymes can reduce various physiologically important heterocyclic enones, unsaturated esters, and imines, which are inert to other enzymes.[5,10,31,32] Recently, it was shown that F_{420}-dependent reductases (FDR), part of the split β-barrel fold FDORs, can reduce α,β-unsaturated ketones and aldehydes in an enantio- and regioselective fashion and, interestingly, yielding the opposite enantiomer as would be formed by the well-studied FMN-dependent old yellow enzyme-type reductases.[33] Also F_{420}-dependent enantioselective secondary alcohol dehydrogenases were characterized.[23,34] These enzymes could also be used as cofactor recycling systems to supply reductases with reduced F_{420}. The well-studied F_{420}:NADPH oxidoreductases[26,35−39] and sugar-6-phosphate dehydrogenases[27,40−44] could also be used as recycling systems. These enzymes form a biocatalytic toolbox which is anticipated to expand, as many genomes are predicted to accommodate genes for F_{420}-dependent enzymes that have yet to be characterized.[4,29]

The main bottleneck in the application of F_{420}-dependent enzymes thus far is the limited availability of the cofactor. Many of the organisms that produce F_{420} are hard to culture or grow relatively slowly. The best production organism, *Mycobacterium smegmatis*, still only produces 1.4 μmol/L of culture.[45,46] Straightforward organic synthesis cannot be used as an alternative option because of the complicated, heterogeneous molecular structure of the cofactor. Especially, the regioselectivity is very challenging as many groups in, for instance, the ribityl moiety and the poly-γ-glutamyl tail have similar reactivity. Heterologous biosynthesis in faster growing hosts was, until recently, impossible because of some missing links in the F_{420}-biosynthesis pathway. The recent elucidation of the complete biosynthesis pathway made heterologous production of the cofactor in *Escherichia coli* actually possible but—thus far—has the same low yields as with *M. smegmatis*.[47]

Herein we describe the chemoenzymatic production of the unnatural F_{420} analogue FO-5′-phosphate, which we coined FOP. The structure of FOP is analogous to FMN, the cofactor that is used in enzymes that share homology with the TIM barrel fold and split β-barrel-like fold F_{420}-depedent oxidoreductases and that may be the ancestors of F_{420}-dependent oxidoreductases.[9,23,24,41] To generate this functional alternative for F_{420}, the FO core was synthesized, as described by Hossain et al.[48] with small modifications. FO was 5′-phosphorylated with an engineered variant of the riboflavin kinase from *C. ammoniagenes*. Site-directed mutagenesis was applied to the enzyme in order for it to accommodate FO. The enzyme activity with FOP as a coenzyme was tested for a representative member of each structural class of F_{420}-dependent oxidoreductases.[29,41]

MATERIALS AND METHODS

Reagents and chemicals were purchased from Sigma-Aldrich (St. Louis, MO, U.S.A.) unless indicated otherwise. Mutagenic primers were also ordered at Sigma-Aldrich. Ligase, and restriction endonucleases were obtained from New England Biolabs (NEB, Ipswich, MA, U.S.A.). PfuUltra Hotstart PCR Mastermix (Agilent Technologies) was used for mutagenic PCR (QuikChange). Plasmid DNA was isolated using the QIAprep Miniprep Kit, and PCR products were purified with the QIAquick PCR Purification Kit (Qiagen, Valencia, CA, U.S.A.).

F_{420} Production. F_{420} was isolated from *Mycobacterium smegmatis* as described by Bashiri et al. and Isabelle et al.[45,46] The production strain *M. smegmatis* mc^2 4517 was a kind gift from Dr. G. Bashiri from the University of Auckland, New Zealand.

FO and FO-7-Methyl Synthesis. FO was synthesized using the approach described by Hossain et al.[48] with a modification for the reductive amination procedure. These two steps are done in one step via reductive amination with sodium cyanoborohydride, instead of synthesis of the mixture of anomers and then reduction of them. FO-7-Me was synthesized using the same modified procedure as for synthesis of FO. Detailed procedures and physical data can be found in the Supporting Information.

Gene Cloning and Mutagenesis of *C. ammoniagenes* Riboflavin Kinase. The *C. ammoniagenes* riboflavin kinase gene (*CaRFK*) was ordered at GenScript (Piscataway, NJ, U.S.A.), codon optimized for *E. coli*. It was composed of the C-terminal kinase domain of the FAD synthetase gene, *ribF* (NCBI#: D37967.1), previously described by Iamurri et al.[49] The nucleotide sequence and protein sequence are shown in Figures S1 and S2, respectively. The gene was cloned into a pBAD/*Myc*-His vector (Invitrogen, Thermo-Fisher) using restriction sites NdeI and HindIII, following standard cloning procedures.[50] Site-directed mutagenesis was performed on the riboflavin kinase gene with the use of mutagenic primers, degenerate at a chosen codon, using the QuikChange mutagenesis kit (Stratagene), following the procedure of the manufacturer. Primers were designed with the Agilent QuikChange primer design tool (http://www.genomics.agilent.com/primerDesignProgram.jsp). The used primers are listed in Table S1. Sequencing was performed at GATC (Constanz, Germany). The plasmids were transformed into calcium chloride chemically competent *E. coli* NEB 10-beta (New England Biolabs Ipswich, MA, U.S.A.) for amplification and protein expression, using standard protocols.[50]

Expression and Purification of *C. ammoniagenes* Riboflavin Kinase. An *E. coli* NEB 10-beta overnight culture in Terrific broth (TB), supplemented with 50 μg mL^{-1} ampicillin, was grown at 37 °C, 135 rpm. The overnight culture was diluted a hundred times in 200 mL of fresh TB with 50 μg mL^{-1} ampicillin in a 500 mL Erlenmeyer flask. This was grown at 37 °C, 135 rpm until the OD_{600} reached ∼0.5, at which the culture was induced with 0.2% L-arabinose and further grown at 17 °C for 36 h. Cells were harvested by centrifugation at 4000*g* for 20 min at 4 °C. The cell pellets were stored at −20 °C until purification. Cell pellets were resuspended in about 10 mL of 50 mM Tris/HCl pH 8.0, 200 mM NaCl, 10 mM imidazole, 1 mM β-mercaptoethanol, and

DOI: 10.1021/acscatal.9b01506
ACS Catal. 2019, 9, 6435−6443

cOmplete mini EDTA-free Protease Inhibitor Cocktail. The cells were lysed by sonication, using a Sonics Vibra-Cell VCX 130 sonicator with a 3 mm stepped microtip (5s on, 10s off, 70% amplitude, 7.5 min). Cell debris were pelleted by centrifugation at 8000*g* for 40 min at 4 °C. The clear supernatant was incubated on 2 mL of Ni-Sepharose High Performance (GE Healthcare, Eindhoven, The Netherlands) for 12 h at 4 °C, with gentle shaking. The column was washed extensively with 3 column volumes of 50 mM Tris/HCl pH 8.0, 200 mM NaCl, 20 mM imidazole, and the protein was eluted with 50 mM Tris/HCl pH 8.0, 200 mM NaCl, 300 mM imidazole. The eluted protein was then desalted and concentrated using Amicon Ultra centrifugal filter units with a 3 kDa molecular weight cutoff, exchanging the buffer with 50 mM Tris/HCl pH 8.0, 200 mM NaCl. The protein was flash-frozen in liquid nitrogen and stored at −80 °C until further use. Purity was checked with SDS-PAGE analysis, and protein concentrations were measured by Bradford analysis, using the standard protocols.

Expression and Purification of F_{420}-Dependent Enzymes. Genes, plasmids, and host strains were already in the collection of this lab from earlier studies. *T. fusca* F_{420}:NADPH oxidoreductase (TfuFNO) was expressed and purified as described by Kumar and Nguyen et al.[26] *R. jostii* RHA1 F_{420}-dependent glucose-6-phosphate dehydrogenase (RHA1-FGD) was expressed and purified as described by Nguyen et al.[27] The sugar-6-phosphate dehydrogenase from *C. arvum* (FSD-Cryar) was expressed and purified as described by Mascotti and Kumar et al.[41] The F_{420}-dependent reductases from *M. hassiacum* (FDR-Mha) and *R. jostii* RHA1 (FDR-RHA1) were expressed and purified as described by Mathew and Trajkovic et al.[33]

Riboflavin Kinase Activity Assay and HPLC Analysis. The activity of wild-type CaRFK and mutant enzymes toward riboflavin and FO was measured in conversion experiments. Conversion mixtures contained 1 μM enzyme and 50 μM riboflavin, FO-7-methyl (FO-7-Me) or FO in 50 mM Tris/HCl pH 8, 100 mM $MgCl_2$, 10 mM ATP. The reaction mixtures with a total volume of 0.5 mL were incubated at room temperature or 37 °C for 12 h. Samples were taken either at certain intervals (0, 5, 10, 15, 30 min) or after 12 h. Conversions were measured by either high-performance liquid chromatography (HPLC) or thin layer chromatography (TLC). The TLC method was previously described by Iamurri et al.[49] The HPLC method was a modified version of that of Iamurri et al. The reactions were quenched with 100% formic acid (FA), 1:5 FA:sample, incubating on ice for 5 min. Then, the samples were spun down at 8000*g* in a table top centrifuge at 4 °C and neutralized with 1.6 mM NaOH, 1:9 NaOH:sample. Supernatant (100 μL) was used for HPLC analysis. Samples were separated on an Alltech Alltime HP C18 5 μ, 250 mm column by applying a linear gradient of 50 mM ammonium acetate pH 6.0 with 5% acetonitrile (buffer A) and 100% acetonitrile (buffer B): *t* = 0 min/100:0 (A:B), *t* = 20 min/75:30 (A:B), *t* = 30 min/5:95 (A:B), *t* = 35 min/5:95 (A:B), *t* = 40 min/75:30 (A:B), *t* = 45 min/100:0 (A:B). The separation was monitored in time at 262 nm. The retention times for FO, FOP, FO-7-Me, and FO-7-Me-P are 17, 15, 21, and 19 min, respectively.

Chemoenzymatic Synthesis of FOP. CaRFK F21H F85H A66I (10 μM) was added to 50 μM FO in 50 mL of 50 mM Tris/HCl pH 8, 100 mM $MgCl_2$, 10 mM ATP and was incubated at room temperature for 24 h. The reaction mixture was spun down at 8000*g* in a table top centrifuge and applied to a Reveleris C18-WP Flash cartridge column. FOP was eluted with deionized water, and purity was verified by HPLC, as described above. The product was concentrated by water evaporation under reduced pressure with a rotary evaporator. FOP was either kept at −20 °C for long-term storage or at 4 °C for short-term storage. Obtained FOP was confirmed by HRMS (result is shown in Supporting Information).

Steady-State Activity Assays for Selected F_{420}-Dependent Enzymes with FO, FOP, and F_{420}. The Michaelis−Menten kinetic parameters for TfuFNO with FO and FOP were obtained by the spectrophotometric assay as described by Kumar and Nguyen et al.[26] In short, the measurements were performed at 25 °C by adding 25−50 μM enzyme to 50 mM KPi, pH 6.0, with a constant NADPH concentration of 250 μM and varying concentrations of FO and FOP between 0.625 and 50 μM. The activity of RHA1-FGD and FSD-Cryar with FO, F_{420} and FOP was obtained by the spectrophotometric assay as described by Nguyen et al.[27] and Mascotti and Kumar et al.,[41] respectively. Glucose-6-phosphate was used as substrate at a constant concentration of 20 mM. The concentration of FO, FOP, and F_{420} was varied between 1.25 and 50 μM in the appropriate Tris/HCl-based buffers for each enzyme at 25 °C.[27,41]

The absorbance at 400 nm was followed in time for all the experiments, and observed slopes (k_{obs}) were calculated with ε_{400} (F_{420}) = 25.7 mM^{-1} cm^{-1}. All experiments were performed in triplicates. The k_{obs} values were plotted against de FO/FOP/F_{420} concentration, and the data was fitted to the Michaelis−Menten (eq 1) or Hill equation (eq 2) by nonlinear regression, using GraphPad Prism v. 6.0 (GraphPad Software Inc., La Jolla, CA, U.S.A.).

$$k_{obs} = \frac{k_{cat}\cdot[S]}{K_m + [S]} \quad (1)$$

$$k_{obs} = \frac{k_{cat}\cdot[S]^h}{K_{half}{}^h + [S]^h} \quad (2)$$

The kinetic parameters for the F_{420}-dependent reductase FDR-Mha were obtained as follows: $FOPH_2$ and $F_{420}H_2$ were prepared by incubating 500 μM FOP or F_{420} with 10 μM FSD-Cryar and 20 mM glucose-6-phosphate in 50 mM Tris/HCl, pH 8.0, until the yellow color disappeared. Then, the mixture was passed through an Amicon Ultra 0.5 mL centrifugal filter, 10 kDa molecular weight cutoff. The filtrate, containing 500 μM $FOPH_2$ or $F_{420}H_2$, was then immediately used for a spectrophotometric assay. The assay mixture contained 0.1−1 μM FDR-Mha, 1.0 mM 2,6,6-trimethyl-2-cyclohexene-1,4-dione, and various concentrations of $FOPH_2$ and $F_{420}H_2$ between 1.25 and 50 μM in 50 mM Tris/HCl, pH 8.0. The increase in absorbance at 400 nm was measured in time over several minutes. The k_{obs} values were calculated using ε_{400} (F_{420}) = 25.7 mM^{-1} cm^{-1}. All experiments were performed in triplicates at 25 °C. Kinetic data was analyzed by nonlinear regression and fitted to the Hill equation for cooperative binding (eq 2), using GraphPad Prism v. 6.0 (GraphPad Software Inc., La Jolla, CA, U.S.A.).

Conversion Experiments with F_{420}-Dependent Reductases from *M. hassiacum* and *R. jostii* RHA1 with FO, FOP, and F_{420}. The reaction mixture contained 400 μL of 50 mM Tris/HCl pH 8.0 supplemented with 1.0 mM cinnamaldehyde, 20 μM FO/FOP/F_{420}, 1.0 μM TfuFNO, 10

DOI: 10.1021/acscatal.9b01506
ACS Catal. 2019, 9, 6435−6443

mM NADPH, 25 μM FDR-RHA1/FDR-Mha, and DMSO (3% v/v). The reaction was performed in a closed 1 mL glass vial in the dark at 25 °C and 135 rpm for 3 h. The reaction was quenched by adding the mixture to an equal amount of acetonitrile and then incubated on ice for 5 min. This mixture was spun down at 8000*g* in a table top centrifuge at 4 °C, and 100 μL supernatant was used for analysis on HPLC. The depletion of substrate and formation of product were analyzed at 240 nm, using an isocratic mobile phase of 60:40 water:acetonitrile on an Alltech Alltime HP C18 5μ, 250 mm column.

RESULTS

Engineering of *C. ammoniagenes* Riboflavin Kinase toward Activity on FO. The C-terminal riboflavin kinase domain (CaRFK) of the FAD synthetase (RibF) from *C. ammoniagenes*, previously described by Iamurri et al.[49] and Herguedas et al.,[51] was chosen for the biocatalytic 5′-phosphorylation of FO. The truncated *ribF* gene (NCBI#: D37967.1), *CaRFK*, was ordered, codon optimized for *E. coli* and was transformed into *E. coli* NEB 10-beta as a pBAD-*CaRFK* construct, equipped with a C-terminal 6× histidine tag. Purification of the respective protein, CaRFK, was achieved by table-top nickel affinity chromatography, yielding about 20 mg L^{-1} pure CaRFK.

Conversion experiments with 50 μL of FO and 1−50 μM CaRFK, analyzed by reverse-phase HPLC after 12 and 48 h at 20 or 37 °C, showed that the wild-type enzyme had no detectable activity toward FO. Therefore, structure-guided site-directed mutagenesis was performed. The crystal structure of the C-terminal riboflavin kinase domain of RibF, PDB ID 5A89,[51] was used to identify suitable sites for mutagenesis. Polar amino acids were introduced at positions 21, 85, and 122 with QuikChange-PCR to accommodate the 8-hydroxyl group of FO (numbering according to the protein sequence given in Figure S2). Single-point mutations, as well as double mutations, however, did not result in any activity toward FO. Yet, interestingly, the apparent activity toward another deazaflavin, FO-7-methyl (8-demethyl-8-hydroxy-5-deazariboflavin, a molecule that is structurally halfway riboflavin and FO), was increased by these mutations, while the activity toward RF was significantly diminished (see Figure 2).

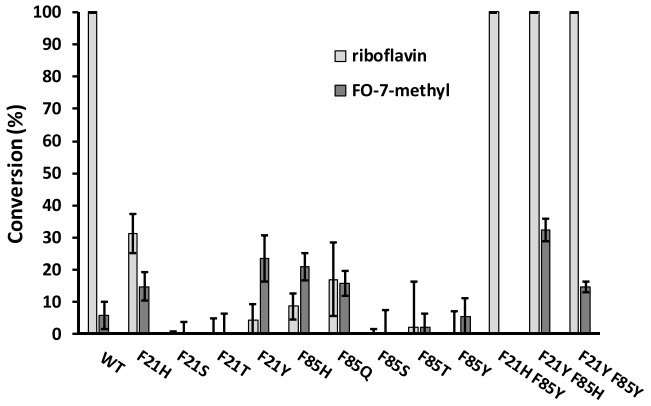

Figure 2. Conversion of riboflavin and FO-7-methyl by single and double CaRFK mutants within 12 h of incubation at 37 °C. Enzyme concentrations are 17 μM for single mutants and 1 μM for double mutants. Experiments were performed in duplicates. Error bars represent standard deviations.

Gratifyingly, introduction of three mutations resulted in activity on FO: mutations A66 V/A66I, together with F21H/Y and F85H/Y yielded FO conversions of 61 to 81% in 12 h (see Figure 3). Replacing alanine at position 66 by a

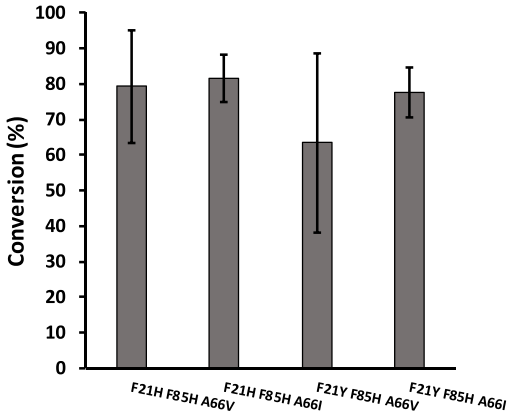

Figure 3. Conversion of FO to FOP within 12 h of incubation at 37 °C with several CaRFK mutants. Experiments were performed in duplicates. Error bars represent standard deviations.

valine or isoleucine might fill up the void that was left vacant by the missing 7-methyl group in FO, making it impossible for water to reside there. Introduction of additional polar residues at position 122 and the mutation T23S, both in the same binding pocket facing the 8-hydroxyl group of FO, did not increase the activity any further.

Chemoenzymatic Synthesis of FO-7-Me-P and FOP. Incubating 50 μM FO-7-Me with 10 μM F21Y/F85H CaRFK mutant or FO with 10 μM F21H/F85H/A66I CaRFK mutant in a volume of 50 mL resulted in full conversion of FO-7-Me to FO-7-Me-P and FO to FOP within 24 h at 37 °C. The product could be purified from the other reaction components with the aid of a preparative reverse-phase liquid chromatography and was concentrated by rotary evaporation under reduced pressure. The yield of 50 mL of reaction volume was about 1 mg (2.5 μmol) of FOP and FO-7-Me-P, in a final concentration of about 400 μM (measured by absorbance at 400 nm, ε_{400} = 25.7 mM^{-1} cm^{-1}). Obtained FO-7-Me-P and FOP were confirmed by HRMS (see Supporting Information).

Purification of F_{420}-Dependent Oxidoreductases. The F_{420}:NADPH oxidoreductase from *T. fusca* (TfuFNO) was expressed and purified as described by Kumar and Nguyen et al.[26] with a yield of approximately 140 mg L^{-1} pure protein. The glucose-6-phosphate dehydrogenase from *R. jostii* RHA1 (RHA1-FGD) and the sugar-6-phosphate dehydrogenase from *C. arvum* (FSD-Cryar) were expressed and purified as described by Nguyen et al.[27] and Mascotti and Kumar et al.,[41] respectively. Yields of purified enzyme were similar as described by the papers mentioned above. Similar results were also obtained for the expression and purification of the F_{420}-dependent reductases from *M. hassiacum* (FDR-Mha) and *R. jostii* RHA1 (FDR-RHA1), as described by Mathew and Trajkovic et al.[33]

Steady-State Kinetics Using FOP as Alternative Cofactor. The activity of the F_{420}-dependent enzymes TfuFNO, RHA1-FGD, FSD-Cryar, and FDR-Mha toward FO, FOP, and F_{420} was measured spectrophotometrically. Steady-state kinetic parameters were measured by varying the concentration of the coenzymes FO, FOP, and F_{420}, while

DOI: 10.1021/acscatal.9b01506
ACS Catal. 2019, 9, 6435−6443

Table 1. Steady-State Kinetic Parameters with Three Different Deazaflavin Cofactors

enzyme	cofactor	k_{cat} (s^{-1})	K_m or K_{half} (h) (μM)	k_{cat}/K_m (M^{-1} s^{-1})	$\frac{k_{cat}}{K_m}$, $F_{420}/\frac{k_{cat}}{K_m}$, FOP
TfuFNO	F_{420}	3.3[a]	2.0[a]	1.7×10^6	2.0
	FOP	3.3	4.0[b] (1.8)	8.3×10^5	
	FO	2.2	4.8[b] (2.9)	4.6×10^5	
FSD-Cryar	F_{420}	33.0	13.6	2.4×10^6	12.6
	FOP	1.3	7.0	1.9×10^5	
	FO	-	-	-	
FDR-Mha	F_{420}	1.8×10^{-2}	12.1[b] (4.4)	1.5×10^4	22.4
	FOP	1.3×10^{-2}	19.3[b] (2.9)	6.7×10^2	
	FO	-	-	-	

[a]Values described by Kumar et al.[26] [b]K_{half} values, according to eq 2, Hill coefficients (h) are given in between brackets Errors are within a 10% range.

keeping the other substrates at constant, saturating concentrations. The slopes of absorbance decrease—or increase in the case of FDR-Mha—at 400 nm were measured, and the observed rates (k_{obs}) were calculated using ε_{400} = 25.7 mM^{-1} cm^{-1}. The observed rates were plotted against the cofactor concentration and fitted to the Michaelis−Menten or the Hill model for positive cooperativity (eqs 1 and 2, respectively).

Tfu-FNO showed activity with all three tested deazaflavins (FO, FOP, and F_{420}). The kinetic data with FO and FOP did not fit well to the Michaelis−Menten kinetic model but could be fitted to a Hill plot for cooperative substrate binding kinetics (Figures S4 and S5). This positive cooperativity can be explained by the dimeric structure of the enzyme. Cooperativity was also observed for the FNO from *Archaeoglobus fulgidus*, using NADPH and FO, as reported by Le et al.[52] Strangely, positive cooperativity was not seen with F_{420} as a coenzyme, as discussed by Kumar and Nguyen et al.[26] The kinetic parameters for FO and FOP, however, are similar to that of F_{420} (see Table 1). Thus, FO, FOP and F_{420} are all equally well used as coenzymes in NADPH oxidation by TfuFNO. The crystal structure of TfuFNO (PDB ID 5N2I),[26] superimposed with the crystal structure of the F_{420}-bound FNO homologue from *A. fulgidus* (1JAY),[28,39] shows that only the FO part of F_{420} is bound and that the rest of the molecule is actually located outside of the enzyme. Therefore, the phosphate of FOP or phospho-L-lactyl and poly-γ-glutamyl tail of F_{420} have only minor contributions to the binding affinity.

It was found that RHA1-FGD shows no activity with FO or FOP, while it has a k_{cat} of 17 s^{-1} and K_m of 3.8 μM for F_{420}.[27] The crystal structure of RHA1-FGD (PDB ID 5LXE),[27] superimposed with the F_{420}-bound crystal structure of the *M. tuberculosis* homologue (PDB ID 3Y4B),[25] shows that the first glutamate moiety of the F_{420} poly-γ-glutamyl tail forms hydrogen bonds with the protein backbone. This could be the reason for being unable to use FO or FOP as coenzyme, which are lacking the glutamyl tail. FSD-Cryar, however, with 57% sequence identity to RHA1-FGD, did show detectable activity toward FOP. The k_{obs} data fitted well to a Michaelis−Menten curve and gave a k_{cat} of 1.3 s^{-1} and K_m of 7.0 μM for FOP (Figures S6 and S7, Table 1). Both values are lower than the kinetic parameters measured for the native cofactor F_{420}, being 33 s^{-1} and 13.9 μM for the k_{cat} and the K_m, respectively (Table 1). Although the K_m values are in the same range ($K_{m,FOP}$ is ∼2 times lower than $K_{m,F420}$), the k_{cat} value for F_{420} is 25 times higher than that for FOP. The catalytic efficiency for FOP, however, is only 1 order of magnitude lower than that when using F_{420}. The measured k_{obs} values for different concentrations of FO could not be fitted with the formula for the Michaelis−Menten model. A good fit could be obtained with a sigmoidal function, but the plateau was never reached with FO concentrations up to 80 μM. Higher concentrations could not be tested because of the solubility of FO in buffer. Although the data could not be used to calculate the kinetic parameters of FSD-Cryar with FO, it is safe to say that the K_m must be significantly higher than that of FOP and F_{420}. The k_{obs} at a concentration of 80 μM FO, the highest concentration tested, is about 20% of the k_{cat} with FOP (see Figure S8).

The kinetic parameters could also be established for FDR-Mha with both FOP and F_{420} as coenzymes. But the kinetic parameters for FO, however, could not be measured. The reduced form of this deazaflavin could not be obtained as it could not be reduced by FSD-Cryar or RHA1-FGD. TfuFNO, which can reduce FO, could not be used as the necessary excess of NADPH would interfere with the FO absorbance at 400 nm. The k_{obs} data for both F_{420} and FOP fitted well to a sigmoidal Hill-curve (eq 2; Figures S9 and S10). This could mean positive cooperativity or the fact that the lower concentrations of the coenzymes were in the same range as the enzyme concentration, so not being present in saturating conditions and, thus, not fitting to the Michaelis−Menten model. The same sigmoidal behavior was also seen for the activity of enzymes of the same structural fold class in *M. smegmatis*, denoted MSMEG_3356 and MSMEG_3380, with various concentrations of F_{420}.[5] The asymptotes to the plateau values of the curves still give a good description of the k_{cat}, and the K_{half} still gives an accurate estimation for coenzyme specificity. From Table 1, it can be seen that FOP has a somewhat lower k_{cat} and higher K_m value than F_{420}, but they are still in the same range.

Conversion Experiments with FDR-Mha and FDR-RHA1. Since the catalytic parameters could not be determined spectrophotometrically for FDR-Mha and FO, conversion experiments were used to compare the activity of FDR-Mha and FDR-RHA1 with FO, FOP, and F_{420}. The conversion of cinnamaldehyde was measured by reverse-phase HPLC after 3 h of incubation for all three coenzymes at concentration of 20 μM. The results show that the conversion of cinnamaldehyde is around 70% when using F_{420} for both FDR-Mha and FDR-RHA1. The conversion when using FOP is close to 40%, which is in line with the spectrophotometric experiments. The conversion of cinnamaldehyde with FO as a coenzyme is lower than that of FOP by about 10 to 18 percentage points. These results show that the apparent activity follows the trend F_{420} > FOP > FO (see Figure 4).

DOI: 10.1021/acscatal.9b01506
ACS Catal. 2019, 9, 6435−6443

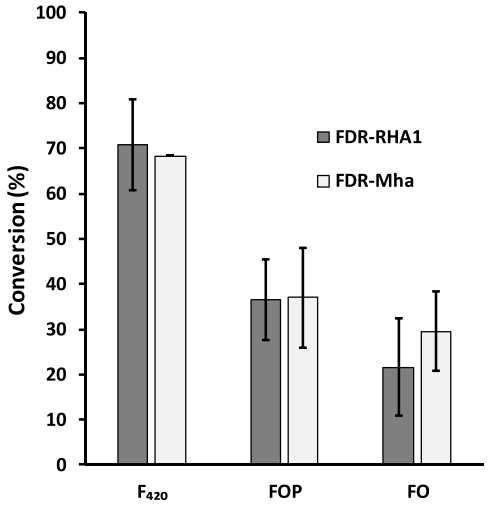

Figure 4. Conversion of cinnamaldehyde within 3 h of incubation at 25 °C by FDR-Mha and FDR-RHA1, using FO, FOP, and F_{420} as coenzymes. Experiments were performed in duplicates. Error bars represent standard deviations.

DISCUSSION

Enzymes that utilize F_{420} could become a biotechnological tool of importance in the near future. The very low redox potential of the cofactor can be utilized for the bioconversion of compounds that would otherwise be recalcitrant to enzymes.[5,10,21,32] The now known F_{420}-dependent reductases and cofactor recycling systems harbor interesting activities for biocatalysis.[29,30] Genome studies revealed that many bacteria and archaea contain putative F_{420}-dependent enzymes that yet have to be characterized[3−5] and could potentially yield new biocatalysts with novel interesting properties.

A bottleneck for application of F_{420}-dependent enzymes is the low availability of the cofactor, as many F_{420}-producing organisms are slow-growing and hard to culture, resulting in low yields.[45,46] Furthermore, the complex structure of the cofactor prevents straightforward chemical synthesis methods. The recent and remarkable efforts by Bashiri et al.[47] to heterologously produce F_{420} in *E. coli* unfortunately still resulted in similar low yields as with *M. smegmatis*. This inspired us to synthesize a F_{420} analogue that could replace F_{420}.

The crystal structures of F_{420}-dependent oxidoreductases show that these enzymes can mainly be divided into three distinct structural classes, namely, the Rossmann fold, TIM barrel fold, and the split β-barrel-like fold class.[27,29,41] The same crystal structures also show that the major part of the poly-γ-glutamyl tail of the cofactor is not bound by the enzyme.[9,23,24,26−28] The main interactions between F_{420} and the enzyme are formed by the FO core structure and the phosphate group, whereas the lactyl group and poly-γ-glutamyl tail form less interactions. The TIM barrel fold and the split β-barrel like fold classes share structural homology with FMN-dependent oxidoreductases, which can explain this observed cofactor-enzyme binding pattern. Furthermore, it was recently shown by Mascotti and Kumar et al.[41] that the TIM barrel fold clade probably has evolved from a FMN-dependent enzyme. Therefore, we proposed FOP, 7,8-didemethyl-8-hydroxy-5-deazariboflavin-5′-phosphate, as an alternative for F_{420}. It is worth noting that FOP is not a naturally occurring cofactor and is also not an intermediate in the biosynthesis of F_{420}. Chemical hydrolysis of F_{420}, in order to elucidate the structure of this cofactor by Eirich et al., however, produced FOP.[20] The authors then coined the term F+ for this deazaflavin compound.

The FO core structure was synthesized by a straightforward organic synthesis procedure. Similar to the biosynthesis of FMN from riboflavin, the phosphate group was then attached enzymatically at the 5′-position with the aid of an tailor-made kinase. A riboflavin kinase (RFK) was used as starting point to engineer a FO kinase since the catalytic core structure, FO, is structurally very similar to that of riboflavin. The RFK from *C. ammoniagenes*, obtained by truncation of the bifunctional FAD synthetase, RibF, was chosen as it was already well-studied by Iamurri et al.[49] Previous research on the enzyme showed its ease of expression and purification and the remarkable range of riboflavin analogues that could be converted, including 5-deazariboflavin. Unfortunately, we discovered that RFK does not accept FO as substrate. Therefore, structure-inspired site-directed mutagenesis was employed to accommodate the more hydrophilic FO in the active site. Introduction of polar residues at position 21 and 85 could facilitate the hydroxyl-group of FO in an otherwise hydrophobic binding pocket. Substitutions of the phenylalanines at these positions by tyrosine and histidine yielded the most active biocatalysts. Substitution of alanine by valine or isoleucine at position 66 was crucial for introducing activity toward FO, probably to fill the space left vacant by the 7′-methyl group that is absent in FO. With these triple mutants conversion of FO into FOP could be achieved. Structure-based site-directed mutagenesis on *C. ammoniagenes* RFK can thus expand the already large substrate acceptance of riboflavin analogues even more, making it a useful tool for the synthesis of unnatural (deaza)flavin cofactors.

The drawback of using riboflavin kinase is its low stability,[49] which prevents the use of cosolvents. Since the solubility of FO and other riboflavin analogues in water is quite low, relatively large reaction volumes have to be used for the production of large amounts of phosphorylated compounds. A more stable RFK could be a solution to this problem, if one would like to produce FOP or other cofactors on plant scale. Still, a 50 mL reaction resulted in the production of about 1 mg (2.5 μmol) FOP within 24 h, which translates to a production of 50 μmol/L. Thus, far more than the F_{420} yield from *M. smegmatis*, being 1.4 μmol/L of culture, grown over several days.

The activity of an F_{420}-dependent oxidoreductase from each structural class with FO, FOP, and F_{420} was measured. Steady-state parameters could be determined with FOP and F_{420} for a member of each class, spectrophotometrically. Experiments with the F_{420}:NADPH oxidoreductase from *T. fusca*, TfuFNO, a member of the Rossmann fold structural class, showed that the kinetic parameters for FO, FOP, and F_{420} are in the same range. The K_m values of FO and FOP are slightly higher, resulting in a slightly lower catalytic efficiency that is 3.7 (FO) or 2 (FOP) times lower than that for F_{420}. The similarity in kinetic parameters can be explained by the fact that only the FO core is bound to the enzyme, as can be seen in crystal structures.[26,28]

Members from the TIM barrel fold class showed a significant decrease in activity when FO and FOP were used as coenzymes. The F_{420}-dependent glucose-6-phosphate dehydrogenase from *R. jostii* RHA1 shows no detectable activity at all for the alternative deazaflavin cofactors. The sugar-6-phosphate dehydrogenase from *C. arvum* has activity toward FOP. Although the K_m values for both FOP and F_{420}

DOI: 10.1021/acscatal.9b01506
ACS Catal. 2019, 9, 6435−6443

are similar, the k_{cat} for F_{420} is significantly higher than that of FOP. Still, the catalytic efficiency with FOP is only 1 order of magnitude lower, meaning that the activity with FOP is significant and that FOP could be used as an alternative non-natural cofactor for this enzyme. An ever lower activity was found for FO, indicating that the phosphate moiety of the F_{420} cofactor is important for recognition and/or productive coenzyme binding.

The kinetic parameters for both FDR-MHA1 and FDR-Mha, both members of the split β-barrel fold class for F_{420} and FOP revealed that the K_m and k_{cat} values are in the same order of magnitude, although the catalytic efficiency is 22 times higher for F_{420} than for FOP. It shows that members of this group of F_{420}-dependent enzymes, dedicated to perform reductions, also can utilize the non-natural deazaflavin cofactor that lacks the lactyl-poly glutamyl moiety. No steady-state kinetic parameters could be obtained with the reduced form of FO because the sugar-6-phosphate dehydrogenases could not be used to prepare reduced FO. We decided to perform comparative conversion experiments with cinnamaldehyde as substrate to probe the efficiency of all three deazaflavin cofactors. Here we could see that cinnamaldehyde conversion with FOP is somewhat less effective than with F_{420}, which is in line with the results from the spectrophotometric assay. The conversions with FO are again lower than that with FOP but in the same range. It shows that all three deazaflavins are accepted by the tested reductases, suggesting that for catalysis only the FO part of the F_{420} cofactor is essential.

The experiments have shown that F_{420}-dependent enzymes of all tested structural classes are active on the non-natural, synthetic deazaflavin cofactor FOP and that the activity is typically higher when compared with its precursor, FO. It seems that in all cases, the phosphate group is important for a higher binding affinity, as seen by a lower K_m, and for a higher catalytic turnover, as seen by a higher k_{cat}. When comparing F_{420} and FOP activities the presence of a poly-γ-glutamyl tail seems to be important for higher cofactor affinities and higher catalytic activity. Interestingly, Ney et al. discovered that the presence of a long poly-γ-glutamyl tail of 5 to 8 glutamate residues indeed lowered the K_m, as compared with a shorter tail of two residues, because of favorable electrostatic interactions between tail and enzyme, but also lowered the k_{cat} and vice versa. The effect of higher k_{cat} with lower cofactor affinity can be explained by higher cofactor exchange rates of enzymes at saturating conditions. Surprisingly, the same effect on k_{cat} and K_m is not seen when the poly-γ-glutamyl tail is completely missing. Perhaps, the properties of the more substituted phosphate diester in F_{420} are more favorable for enzyme binding than that of the phosphate monoester in FOP.

The findings of this research show that FOP could also be used as an alternative deazaflavin cofactor in vivo. With having an engineered FO kinase, the introduction of a biosynthetic route toward FOP is feasible. A great advantage of FOP over FO is that it retains inside a cell because of the charged phosphate group, similar to the conversion of riboflavin into FMN. Also, the solubility is enhanced by the addition of a phosphate group. Although the activity for FOP is lower than that for F_{420}, it is still sufficient enough for the use as a cofactor in biocatalysis, as can be seen by the relatively small differences in catalytic efficiency. The ease of production and higher product yields of the cofactor could make up for the decrease in activity when used as coenzyme in F_{420}-dependent enzyme reactions. Therefore, FOP could be the key to successful implementation of F_{420}-dependent enzymes as biocatalytic tools in industry.

■ ASSOCIATED CONTENT

Supporting Information

The Supporting Information is available free of charge on the ACS Publications website at DOI: 10.1021/acscatal.9b01506.

Protein and nucleotide sequence of codon optimized CaRFK, as well as the mutagenic primers used to create point mutations in the *CaRFK* gene; synthesis of FO and FO-7-Me and all the NMR and HRMS spectra for product and intermediate characterization and identification; and all graphs from steady-state kinetic analysis of the F_{420}-dependent enzymes with F_{420}/FOP/FO (PDF)

■ AUTHOR INFORMATION

Corresponding Author

*E-mail: m.w.fraaije@rug.nl.

ORCID

Milos Trajkovic: 0000-0001-7264-1630

Marco W. Fraaije: 0000-0001-6346-5014

Notes

The authors declare no competing financial interest.

■ REFERENCES

(1) Cheeseman, P.; Toms-Wood, A.; Wolfe, R. S. Isolation and properties of a fluorescent compound, factor 420, from *Methanobacterium* strain M.o.H. *J. Bacteriol.* **1972**, *112*, 527−531.

(2) Daniels, L.; Bakhiet, N.; Harmon, K. Widespread distribution of a 5-deazaflavin cofactor in *Actinomyces* and related bacteria. *Syst. Appl. Microbiol.* **1985**, *6*, 12−17.

(3) Ney, B.; Ahmed, F. H.; Carere, C. R.; Biswas, A.; Warden, A. C.; Morales, S. E.; Pandey, G.; Watt, S. J.; Oakeshott, J. G.; Taylor, M. C.; et al. The methanogenic redox cofactor F_{420} is widely synthesized by aerobic soil bacteria. *ISME J.* **2017**, *11*, 125.

(4) Selengut, J. D.; Haft, D. H. Unexpected abundance of coenzyme F_{420}-dependent enzymes in *Mycobacterium tuberculosis* and other actinobacteria. *J. Bacteriol.* **2010**, *192*, 5788−5798.

(5) Taylor, M. C.; Jackson, C. J.; Tattersall, D. B.; French, N.; Peat, T. S.; Newman, J.; Briggs, L. J.; Lapalikar, G. V.; Campbell, P. M.; Scott, C.; et al. Identification and characterization of two families of $F_{420}H_2$-dependent reductases from mycobacteria that catalyse aflatoxin degradation. *Mol. Microbiol.* **2010**, *78*, 561−575.

(6) Coats, J. H.; Li, G. P.; Kuo, M. S.; Yurek, D. A. Discovery, production, and biological assay of an unusual flavenoid cofactor involved in lincomycin biosynthesis. *J. Antibiot.* **1989**, *42*, 472−474.

(7) Li, W.; Chou, S.; Khullar, A.; Gerratana, B. Cloning and characterization of the biosynthetic gene cluster for tomaymycin, an SJG-136 monomeric analog. *Appl. Environ. Microbiol.* **2009**, *75*, 2958−2963.

(8) Wang, P.; Bashiri, G.; Gao, X.; Sawaya, M. R.; Tang, Y. Uncovering the enzymes that catalyze the final steps in oxytetracycline biosynthesis. *J. Am. Chem. Soc.* **2013**, *135*, 7138−7141.

(9) Ahmed, F. H.; Carr, P. D.; Lee, B. M.; Afriat-Jurnou, L.; Mohamed, A. E.; Hong, N.; Flanagan, J.; Taylor, M. C.; Greening, C.; Jackson, C. J. Sequence−structure−function classification of a catalytically diverse oxidoreductase superfamily in *Mycobacteria*. *J. Mol. Biol.* **2015**, *427*, 3554−3571.

(10) Lapalikar, G. V.; Taylor, M. C.; Warden, A. C.; Scott, C.; Russell, R. J.; Oakeshott, J. G. $F_{420}H_2$-dependent degradation of aflatoxin and other furanocoumarins is widespread throughout the *Actinomycetales*. *PLoS One* **2012**, *7*, e30114.

(11) Ebert, S.; Rieger, P. G.; Knackmuss, H. J. (1999) Function of coenzyme F_{420} in aerobic catabolism of 2,4,6-trinitrophenol and 2,4-

DOI: 10.1021/acscatal.9b01506
ACS Catal. 2019, 9, 6435−6443

dinitrophenol by *Nocardioides simplex* FJ2−1A. *J. Bacteriol.* **1999**, *181*, 2669−2674.
(12) Heiss, G.; Hofmann, K. W.; Trachtmann, N.; Walters, D. M.; Rouvière, P.; Knackmuss, H. npd gene functions of *Rhodococcus* (*opacus*) *erythropolis* HL PM-1 in the initial steps of 2,4,6-trinitrophenol degradation. *Microbiology* **2002**, *148*, 799−806.
(13) Jirapanjawat, T.; Ney, B.; Taylor, M. C.; Warden, A. C.; Afroze, S.; Russell, R. J.; Lee, B. M.; Jackson, C. J.; Oakeshott, J. G.; Pandey, G.; Greening, C. The redox cofactor F_{420} protects mycobacteria from diverse antimicrobial compounds and mediates a reductive detoxification system. *Appl. Environ. Microbiol.* **2016**, *82*, 6810−6818.
(14) Gurumurthy, M.; Rao, M.; Mukherjee, T.; Rao, S. P.; Boshoff, H. I.; Dick, T.; Barry, C. E.; Manjunatha, U. H. A novel F_{420}-dependent anti-oxidant mechanism protects *Mycobacterium tuberculosis* against oxidative stress and bactericidal agents. *Mol. Microbiol.* **2013**, *87*, 744−755.
(15) Hasan, M. R.; Rahman, M.; Jaques, S.; Purwantini, E.; Daniels, L. Glucose-6-phosphate accumulation in mycobacteria: implications for a novel F_{420}-dependent anti-oxidant defense system. *J. Biol. Chem.* **2010**, *285*, 19135−19144.
(16) Purwantini, E.; Mukhopadhyay, B. Conversion of NO_2 to NO by reduced coenzyme F_{420} protects mycobacteria from nitrosative damage. *Proc. Natl. Acad. Sci. U. S. A.* **2009**, *106*, 6333−6338.
(17) Denny, W. A. TBA-354: a new drug for the treatment of persistent tuberculosis. *Chem. New Zeal.* **2015**, *1*, 18−22.
(18) Stover, C. K.; Warrener, P.; VanDevanter, D. R.; Sherman, D. R.; Arain, T. M.; Langhorne, M. H.; Anderson, S. W.; Towell, J. A.; Yuan, Y.; McMurray, D. N.; et al. A small-molecule nitroimidazopyran drug candidate for the treatment of tuberculosis. *Nature* **2000**, *405*, 962−966.
(19) Matsumoto, M.; Hashizume, H.; Tomishige, T.; Kawasaki, M.; Tsubouchi, H.; Sasaki, H.; Shimokawa, Y.; Komatsu, M. OPC-67683, a nitrodihydro-imidazooxazole derivative with promising action against tuberculosis in vitro and in mice. *PLoS Med.* **2006**, *3*, e466.
(20) Eirich, L. D.; Vogels, G. D.; Wolfe, R. S. Proposed structure for coenzyme F_{420} from *Methanobacterium*. *Biochemistry* **1978**, *17*, 4583−4593.
(21) Walsh, C. Naturally occurring 5-deazaflavin coenzymes − biological redox roles. Acc. *Acc. Chem. Res.* **1986**, *19*, 216−221.
(22) Bashiri, G.; Rehan, A. M.; Sreebhavan, S.; Baker, H. M.; Baker, E. N.; Squire, C. J. Elongation of the poly-γ-glutamate tail of F_{420} requires both domains of the F_{420}: γ-glutamyl ligase (FbiB) of *Mycobacterium tuberculosis*. *J. Biol. Chem.* **2016**, *291*, 6882−6894.
(23) Aufhammer, S. W.; Warkentin, E.; Berk, H.; Shima, S.; Thauer, R. K.; Ermler, U. Coenzyme binding in F_{420}-dependent secondary alcohol dehydrogenase, a member of the bacterial luciferase family. *Structure* **2004**, *12*, 361−370.
(24) Aufhammer, S. W.; Warkentin, E.; Ermler, U.; Hagemeier, C. H.; Thauer, R. K.; Shima, S. Crystal structure of methylenetetrahydromethanopterin reductase (Mer) in complex with coenzyme F_{420}: architecture of the F_{420}/FMN binding site of enzymes within the nonprolyl cis-peptide containing bacterial luciferase family. *Protein Sci.* **2005**, *14*, 1840−1849.
(25) Bashiri, G.; Squire, C. J.; Moreland, N. J.; Baker, E. N. Crystal structures of F_{420}-dependent glucose-6-phosphate dehydrogenase FGD1 involved in the activation of the anti-tuberculosis drug candidate PA824 reveal the basis of coenzyme and substrate binding. *J. Biol. Chem.* **2008**, *283*, 17531−17541.
(26) Kumar, H.; Nguyen, Q.-T.; Binda, C.; Mattevi, A.; Fraaije, M. W. Isolation and characterization of a thermostable F_{420}:NADPH oxidoreductase from *Thermobifida fusca*. *J. Biol. Chem.* **2017**, *292*, 10123−10130.
(27) Nguyen, Q.-T.; Trinco, G.; Binda, C.; Mattevi, A.; Fraaije, M. W. Discovery and characterization of an F_{420}-dependent glucose-6-phosphate dehydrogenase (Rh-FGD1) from *Rhodococcus jostii* RHA1. *Appl. Microbiol. Biotechnol.* **2017**, *101*, 2831−2842.
(28) Warkentin, E.; Mamat, B.; Sordel-Klippert, M.; Wicke, M.; Thauer, R. K.; Iwata, M.; Iwata, S.; Ermler, U.; Shima, S. (2001) Structures of $F_{420}H_2$:NADP$^+$ oxidoreductase with and without its substrates bound. *EMBO J.* **2001**, *20*, 6561−6569.
(29) Greening, C.; Ahmed, F. H.; Mohamed, A. E.; Lee, B. M.; Pandey, G.; Warden, A. C.; Scott, C.; Oakeshott, J. G.; Taylor, M. C.; Jackson, C. J. Physiology, biochemistry, and applications of F_{420}- and Fo-dependent redox reactions. *Microbiol. Mol. Biol. Rev.* **2016**, *80*, 451−493.
(30) Taylor, M.; Scott, C.; Grogan, G. F_{420}-dependent enzymes-potential for applications in biotechnology. *Trends Biotechnol.* **2013**, *31*, 63−64.
(31) Ichikawa, H.; Bashiri, G.; Kelly, W. L. Biosynthesis of the thiopeptins and identification of an $F_{420}H_2$-dependent dehydropiperidine reductase. *J. Am. Chem. Soc.* **2018**, *140*, 10749−10756.
(32) Lapalikar, G. V.; Taylor, M. C.; Warden, A. C.; Onagi, H.; Hennessy, J. E.; Mulder, R. J.; Scott, C.; Brown, S. E.; Russell, R. J.; Easton, C. J.; et al. Cofactor promiscuity among F_{420}-dependent reductases enables them to catalyse both oxidation and reduction of the same substrate. *Catal. Sci. Technol.* **2012**, *2*, 1560−1567.
(33) Mathew, S.; Trajkovic, M.; Kumar, K.; Nguyen, Q.-T.; Fraaije, M. W. Enantio- and regioselective ene-reductions using $F_{420}H_2$-dependent enzymes. *Chem. Commun.* **2018**, *54*, 11208−11211.
(34) Widdel, F.; Wolfe, R. S. Expression of secondary alcohol dehydrogenase in methanogenic bacteria and purification of the F_{420}-specific enzyme from *Methanogenium thermophilum* strain TCI. *Arch. Microbiol.* **1989**, *152*, 322−8.
(35) Berk, H.; Thauer, R. K. Function of coenzyme F_{420}-dependent NADP reductase in methanogenic archaea containing an NADP-dependent alcohol dehydrogenase. *Arch. Microbiol.* **1997**, *168*, 396−402.
(36) de Wit, L.; Eker, A. 8-Hydroxy-5-deazaflavindependent electron transfer in the extreme halophile *Halobacterium cutirubrum*. *FEMS Microbiol. Lett.* **1987**, *48*, 121−125.
(37) Dudley Eirich, L. D.; Dugger, R. S. Purification and properties of an F_{420}-dependent NADP reductase from *Methanobacterium thermoautotrophicum*. *Biochim. Biophys. Acta, Gen. Subj.* **1984**, *802*, 454−458.
(38) Elias, D. A.; Juck, D. F.; Berry, K. A.; Sparling, R. Purification of the NADP$^+$:F_{420} oxidoreductase of *Methanosphaera stadtmanae*. *Can. J. Microbiol.* **2000**, *46*, 998−1003.
(39) Kunow, J.; Schwörer, B.; Stetter, K. O.; Thauer, R. K. A F_{420}-dependent NADP reductase in the extremely thermophilic sulfate-reducing *Archaeoglobus fulgidus*. *Arch. Microbiol.* **1993**, *160*, 199−205.
(40) Bashiri, G.; Squire, C. J.; Baker, E. N.; Moreland, N. J. Expression, purification and crystallization of native and selenomethionine labeled *Mycobacterium tuberculosis* FGD1 (Rv0407) using a *Mycobacterium smegmatis* expression system. *Protein Expression Purif.* **2007**, *54*, 38−44.
(41) Mascotti, M. L.; Kumar, H.; Nguyen, Q.-T.; Ayub, M. J.; Fraaije, M. W. Reconstructing the evolutionary history of F_{420}-dependent dehydrogenases. *Sci. Rep.* **2018**, *8*, 17571.
(42) Purwantini, E.; Daniels, L. Purification of a novel coenzyme F_{420}-dependent glucose-6-phosphate dehydrogenase from *Mycobacterium smegmatis*. *J. Bacteriol.* **1996**, *178*, 2861−2866.
(43) Purwantini, E.; Gillis, T. P.; Daniels, L. Presence of F_{420}-dependent glucose-6-phosphate dehydrogenase in *Mycobacterium* and *Nocardia* species, but absence from *Streptomyces* and *Corynebacterium* species and methanogenic Archaea. *FEMS Microbiol. Lett.* **1997**, *146*, 129−143.
(44) Purwantini, E.; Daniels, L. Molecular analysis of the gene encoding F_{420}-dependent glucose-6-phosphate dehydrogenase from *Mycobacterium smegmatis*. *J. Bacteriol.* **1998**, *180*, 2212−2219.
(45) Bashiri, G.; Rehan, A. M.; Greenwood, D. R.; Dickson, J. M.; Baker, E. N. Metabolic engineering of cofactor F_{420} production in *Mycobacterium smegmatis*. *PLoS One* **2010**, *5*, e15803.
(46) Isabelle, D.; Simpson, D. R.; Daniels, L. Large-scale production of coenzyme F_{420}-5,6 by using *Mycobacterium smegmatis*. *Appl. Environ. Microbiol.* **2002**, *68*, 5750−5755.
(47) Bashiri, G.; Antoney, J. P.; Jirgis, E. N. M.; Shah, M. V.; Ney, B.; Copp, J.; Stuteley, S. M.; Sreebhavan, S.; Palmer, B.; Middleditch,

DOI: 10.1021/acscatal.9b01506
ACS Catal. 2019, 9, 6435−6443

M.; Tokuriki, N.; Greening, C.; Baker, E. N.; Scott, C.; Jackson, C. J. A revised biosynthetic pathway for the cofactor F_{420} in prokaryotes. *Nat. Commun.* **2019**, *10*, 1558.
(48) Hossain, M. S.; Le, C. Q.; Joseph, E.; Nguyen, T. Q.; Johnson-Winters, K.; Foss, F. W., Jr. Convenient synthesis of deazaflavin cofactor FO and its activity in F_{420}-dependent NADP reductase. *Org. Biomol. Chem.* **2015**, *13*, 5082−5085.
(49) Iamurri, S. M.; Daugherty, A. B.; Edmondson, D. E.; Lutz, S. Truncated FAD synthetase for direct biocatalytic conversion of riboflavin and analogs to their corresponding flavin mononucleotides. *Protein Eng., Des. Sel.* **2013**, *26*, 791−795.
(50) Sambrook, J.; Green, M. R. *Molecular Cloning: A laboratory manual*, 4th ed.; Cold Spring Harbor Laboratory Press: Cold Spring Harbor, NY, 2012; pp 1−3.
(51) Herguedas, B.; Lans, I.; Sebastián, M.; Hermoso, J. A.; Martinez-Julvez, M.; Medina, M. Structural insights into the synthesis of FMN in prokaryotic organisms. *Acta Crystallogr., Sect. D: Biol. Crystallogr.* **2015**, *71*, 2526−2542.
(52) Le, C. Q.; Oyugi, M.; Joseph, E.; Nguyen, T.; Ullah, M. H.; Aubert, J.; Phan, T.; Tran, J.; Johnson-Winters, K. Effects of isoleucine 135 side chain length on the cofactor donor acceptor distance within $F_{420}H_2$: $NADP^+$ oxidoreductase: A kinetic analysis. *Biochem. Biophys. Rep.* **2017**, *9*, 114−120.

DOI: 10.1021/acscatal.9b01506
ACS Catal. 2019, 9, 6435−6443